RAPID COMMUNICATIONS

PHYSICAL REVIEW B VOLUME 51, NUMBER 15 15 APRIL 1995-I

Exciton dynamics within growth islands of GaAs/$Al_{0.17}Ga_{0.83}As$ single quantum wells

R. Klann and H. T. Grahn
Paul-Drude-Institut für Festkörperelektronik, Hausvogteiplatz 5-7, D-10117 Berlin, Germany

K. Fujiwara
Kyushu Institute of Technology, Tobata, Kitakyushu 804, Japan
(Received 6 December 1994)

We have directly observed the localization dynamics of excitons within growth islands of a GaAs/$Al_{0.17}Ga_{0.83}As$ single quantum well by time-resolved photoluminescence (PL). The PL emission of each growth island is split into two peaks that have an energy separation of 3 meV. These peaks are attributed to the emission of free and localized excitons within the islands. Upon pulsed excitation, the high-energy free-exciton PL line dominates the initial emission, while for longer times (350 ps) the bound-exciton PL peak emerges. This observation directly reflects the localization of free excitons within the growth islands.

The interface quality in molecular-beam epitaxy (MBE) grown GaAs/$Al_xGa_{1-x}As$ semiconductor quantum wells is important in order to realize an ideal two-dimensional (2D) exciton gas. Free 2D excitons are expected to have a large coherence length and a short radiative lifetime of the order of 10 ps.[1,2] However, even at low temperatures most experimental values for the excitonic emission decay time of a single quantum well (SQW) are of the order of 0.25–1 ns. This discrepancy is due to a decrease of the coherence length as a result of scattering at impurities, alloy disorder, and interface roughness, which manifests itself in an inhomogeneous broadening of the exciton emission.[3–13]

By choosing appropriate MBE growth conditions, it is possible to prepare SQW with atomically flat terraces comparable with or even larger than the exciton Bohr radius. In such spatially coherent SQW's, the exciton emission is split into peaks, originating from different monolayer (ML) terraces. This allows the investigation of the exciton dynamics between growth islands by time-resolved photoluminescence (TRPL).[14] The smoothness of the terraces within 1 ML eliminates the contribution of the ML thickness fluctuations to the exciton localization. For this reason the inhomogeneous broadening and the exciton emission dynamics within a single growth island is mainly due to impurities or alloy composition fluctuations.

In this paper, we report on the dynamics of radiative recombination of the lowest heavy-hole exciton of a 3.5-nm SQW with ML growth islands. The exciton dynamics, as monitored by TRPL, is described by a rate equation model. Each ML peak exhibits an additional splitting in two lines separated by 3 meV. These lines are attributed to free and localized excitons within one growth island. We observe the localization of excitons within ML flat growth islands by monitoring the temporal evolution of the luminescence. At early decay times only the free-exciton peak is observed. Within 350 ps this peak disappears and the bound-exciton peak evolves. The energy separation of the time-resolved peaks has the same value as the Stokes shift observed in cw measurements.

The investigated SQW sample is fabricated by MBE with growth interruption at each heterointerface.[15,16] The sample consists of three SQW's with a nominal GaAs thickness of 3.5 nm, 5.5 nm, and 7.8 nm, respectively. In our experiments, we focus on the 3.5-nm SQW which shows the largest PL splitting due to ML growth islands. The SQW's are separated by 36-nm $Al_{0.17}Ga_{0.83}As$ barriers. The QW's are further confined by 0.2-μm-thick $Al_{0.30}Ga_{0.70}As$ layers in order to avoid surface recombination.

Time-integrated PL and PL excitation (PLE) measurements are performed using an intensity stabilized cw Ti:sapphire laser (Coherent 890) tunable between 700 nm and 850 nm as the excitation source. After dispersing the PL with a 1-m monochromator (600 lines/mm grating), a liquid nitrogen cooled charged-coupled-device (CCD) array is used for detection. The PLE signals are detected by a cooled GaAs-photomultiplier. The TRPL experiments are performed using a femtosecond Ti:sapphire laser (Coherent Mira) and a streak-camera system in single shot operation (Hamamatsu C5680). To avoid state filling by carrier accumulation, the repetition rate of the 150 fs full width at half maximum excitation pulses is reduced to 1 MHz by a pulse picker. The excitation light is focused onto the sample with a spot diameter of 150 μm. The density of generated excitons is estimated by the excitation power, the excitation spot size, and the absorption. The emitted luminescence is dispersed by a 22-cm monochromator using a 1200 lines/mm grating and focused onto the photocathode of the streak tube. The streak images are recorded using a cooled CCD array and are further processed by a computer. The spectral resolution is 0.4 nm. The temporal resolution of the single-shot system amounts to 50 ps. The sample is mounted on the cold finger of a He flow cryostat and kept at a temperature of 5.0 K during all experiments.

For the PL and TRPL experiments, the photon energies for excitation are chosen to be nonresonant with respect to the light-hole or higher heavy-hole transitions, but below the $Al_{0.30}Ga_{0.70}As$ confining layers. The excitation pulse creates free carriers within each ML island according to the area ratio of the island sizes. The electron and holes relax to the bottom of the respective bands and form excitons. The fast relaxation process creates an exciton density within each island, which is still proportional to the area distribution of the

0163-1829/95/51(15)/10232(4)/$06.00

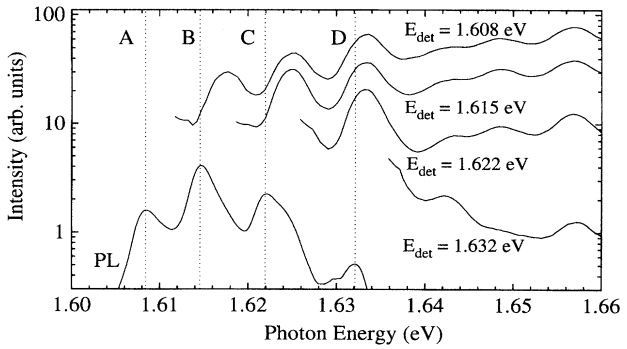

FIG. 1. cw PL and PLE spectra of a 3.5-nm single quantum well (excitation power 0.5 mW, temperature 5 K). The four PL peaks originate from ML islands differing in thickness by 1 ML between 12 ML (D) and 15 ML (A) (excitation energy 1.700 eV). The photon energy of each peak is indicated by a dotted line, which denotes the detection photon energies E_{det} for PLE.

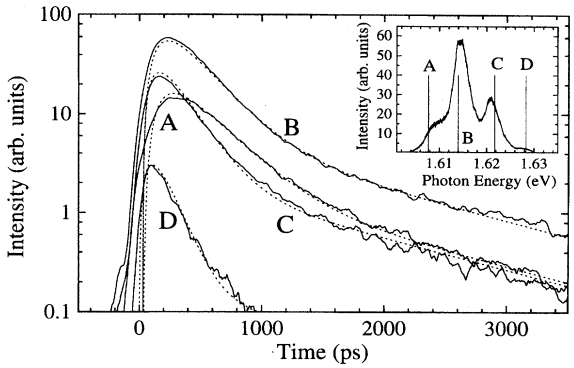

FIG. 2. Temporal evolution of the four ML peaks A–D (full lines) and fit to a rate equation model (dotted line). The excitation energy was 1.676 eV and the temperature was 5 K. The inset shows the time integrated spectra and the spectral position of the four traces.

islands. The free excitons will diffuse to neighboring, wider ML islands or will localize within the respective growth island due to impurities or fluctuations in composition. The emission from the bound-exciton states is redshifted with respect to the free-exciton emission energy by the binding energy, which can be smaller than the energy difference between ML island peaks. Transfer to smaller ML islands is very unlikely due to the low temperature in conjunction with the barrier between the islands. In addition to these relaxation processes, radiative recombination takes place.

The cw PL and PLE spectra of the 3.5-nm SQW are shown in Fig. 1 (excitation power 0.5 mW). We observe four PL peaks which belong to ML islands of 12–15 ML. They are labeled in Fig. 1 as A (15 ML; peak position, 1.608 eV), B (14 ML; peak position, 1.615 eV), C (13 ML; peak position, 1.622 eV) and D (12 ML; peak position, 1.632 eV). PLE spectra with detection energies indicated in the figure are also shown. At higher photon energies the light-hole transitions are observed. The observed Stokes shifts depend on the ML peak varying between 2.5 and 4 meV. The PL signal increases linearly with excitation density. The PL efficiency compares well with the efficiency of a reference sample grown without interruption, thus indicating no additional nonradiative recombination channels due to the different growth conditions.

The interisland transfer is already obvious from the stationary experiments. Comparing the PL and PLE spectra in Fig. 1, we find the largest emission for peak B (14 ML). The largest PLE signal, however, is found for peak D (12 ML). This implies that the thinnest growth island D covers the largest area.[17] Therefore, an efficient transfer to thicker regions of 13–15 ML has to occur within the radiative lifetime. A change of the detection energy with respect to the emission of the four different growth islands (A–D) leaves the PLE spectra unchanged with respect to the heavy-hole transitions.

The interplay between transfer, localization, and emission is visualized by TRPL. After excitation with a 150-fs pulse (photon energy, 1.676 eV; average excitation power, 5 μW; repetition rate, 1 MHz) the temporal evolution of the four different PL peak positions A–D are shown in Fig. 2 (full lines) for times up to 3.5 ns (spectral width 4 meV). The energy positions of A–D are identical to those in Fig. 1. The high-energy PL line D exhibits the fastest decay time. The transfer of excitons to the widest islands A results in a delayed PL signal. The inset shows the spectral position of the four temporal traces. The observed decay for each island peak is described by a biexponential behavior. The fast decay is assigned to free excitons, the slow decay to bound excitons within the island. This interpretation is further confirmed experimentally by temperature dependent TRPL measurements. The free-exciton radiative lifetime increases with increasing temperature. In contrast, the long-living bound-exciton decay time is independent of temperature.

The exciton dynamics is described by a rate equation model including four ML islands, each contain free- and bound-exciton states. In the frame of the model, free excitons can localize within each island, or can recombine radiatively, or they are transferred to wider wells. Bound excitons only recombine radiatively. The free-exciton levels are initially occupied according to the area distribution of the ML islands. The distribution is taken from the ratio of the PLE peaks as $A_A:A_B:A_C:A_D = 0:24:28:48$ (A_i is the area of growth island i, see Fig. 1). Best agreement with the data is obtained with a free-exciton radiative recombination rate of 2.5 ns^{-1} (fast decay component in Fig. 2), an exciton localization rate of 0.67 ns^{-1}, and a bound-exciton radiative recombination rate of 0.74 ns^{-1} (slow decay time). These values are kept constant for all growth islands. The interisland transfer rates agree best with the data for transfer rates from D to C of 5 ns^{-1}, D to B of 30 ns^{-1}, D to A of 10 ns^{-1}, C to B of 1.67 ns^{-1}, and from B to A of 1 ns^{-1}. The transfer rate from C to A is neglected. Cooling of the excitons has been taken into account in the rate equation by a delayed onset of the PL by 50 ps.[18,19] The calculated PL decay is proportional to the sum of the emission rates of free and bound excitons, which are calculated from the product of the exciton density and the respective radiative decay rate (dotted lines in Fig. 2).

This picture of bound and free excitons is further supported by intensity dependent cw PL experiments (Fig. 3).

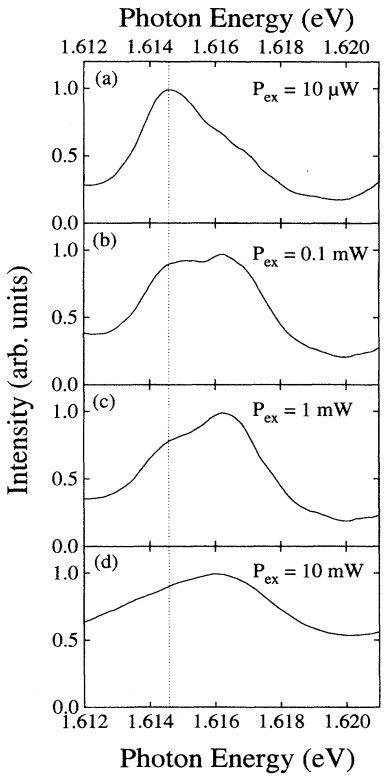

FIG. 3. Intensity dependent normalized cw PL spectra of the 14 ML growth island *B* at 5 K using an excitation energy of 1.664 eV. (a) For a low excitation density of 10 μW the PL peak is located at 1.6146 eV (indicated by the dotted line). (b)–(d) For increasing excitation power the emission spectrum is blueshifted due to filling of the localized exciton states. (b) 0.1 mW, (c) 1 mW, (d) 10 mW.

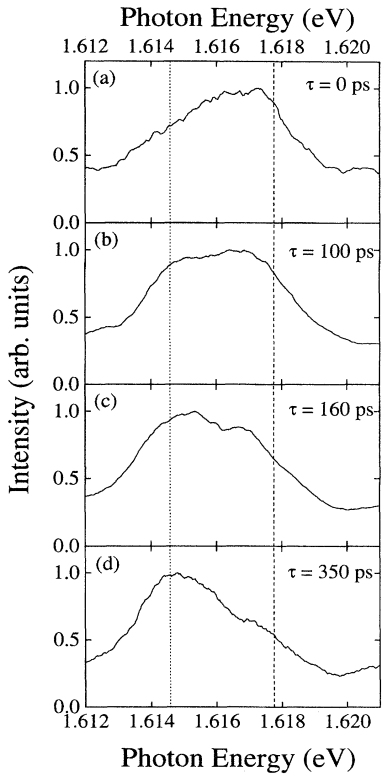

FIG. 4. Normalized PL spectra of the 14 ML growth island peak *B* at different decay times (same energy scale as in Fig. 3). The excitation power of 5 μW creates a density of 1×10^{8} cm^{-2} excitons per pulse (excitation energy 1.715 eV, temperature 5 K). (a) At time 0 ps, (b) at 100 ps, (c) at 160 ps, (d) at 350 ps.

For an excitation intensity of 10 μW [Fig. 3(a)] the PL of the 14 ML island *B* peaks at 1.615 eV (dotted line), i.e., the bound-exciton energy. For an excitation power only ten times higher, a high-energy line arises at 1.617 eV [Fig. 3(b)]. The free-exciton peak at 1.617 eV becomes even more pronounced for 1-mW excitation [Fig. 3(c)]. For the largest excitation density of 10 mW [Fig. 3(d)] the spectrum is broadened due to heating by the excited carriers. The intensity dependent PL spectra demonstrate the state filling of the bound-exciton states with increasing excitation power.

The localization dynamics of free excitons within growth island *B* is directly monitored by TRPL spectra at low excitation densities (Fig. 4). The spectral range is identical to Fig. 3. The spectra are integrated over 50 ps. For a low excitation density of 5 μW (photon energy 1.715 eV) we estimate an exciton density of 1×10^{8} cm^{-2} per pulse. At early times [Fig. 4(a)] the emission is dominated by free excitons, the line peaks at 1.618 eV. This position coincides with the maximum of the PLE spectrum, as indicated by the dashed line. After 100 ps the spectrum splits into a double peak structure with a second peak evolving at 1.615 eV [Fig. 4(b)], the maximum of the cw PL peak (dotted line). The excitons become localized within the growth island and the bound-exciton peak emerges. This behavior is more pronounced after 160 ps where the low-energy peak is even more intense than the high-energy one [Fig. 4(c)]. After 350 ps the low-energy peak is dominant and the high-energy peak is no longer resolved [Fig. 4(d)]. The spectrum is now similar to the cw spectrum in Fig. 3(a). The observation of the evolution of the bound-exciton peak within 350 ps is in excellent agreement with the obtained localization rate of 0.67 ns^{-1}.[20]

The exciton localization dynamics within the atomically flat ML island *B* is directly observed by the temporal evolution of the PL spectrum in addition to a biexponential PL decay behavior. At early times the emission originates from free excitons, because the PL spectrum peaks at the maximum of the PLE spectrum [Fig. 4(a)]. The linewidth of 2 meV of the free-exciton emission within an island is inhomogenously broadened compared to the radiative lifetime of 400 ps. This demonstrates the strong influence of alloy composition fluctuation and impurities to exciton scattering. The relaxation to bound states is directly visualized by the decrease of the free-exciton PL line and the delayed onset of the bound-state exciton emission. The observed spectral positions of the emission peaks at 0 ps and 350 ps coincide with the Stokes shift between PL and PLE. The localization rate of 0.67 ns^{-1} is deduced from a rate equation analysis which also takes into account the transfer rates of free exci-

tons to and from the ML island.

In summary, we have investigated intergrowth and intragrowth island exciton dynamics by TRPL. The splitting of the emission line of a single ML growth island in a free- and bound-exciton peak is observed. TRPL measurements demonstrate the transfer of free excitons between growth islands. Within a single growth island exciton localization to shallow donors is directly monitored by the temporal evolution of the PL spectrum.

We acknowledge valuable discussions with U. Jahn. This work was supported in part by Scientific Research Grant-in-Aid No. 05044109 (Joint Research) from the Ministry of Education, Science and Culture of Japan.

[1] V. Srinivas, J. Hryniewicz, Y. Chen, and C. Wood, Phys. Rev. B **46**, 10 193 (1992).

[2] D. Citrin, Phys. Rev. B **47**, 3832 (1993).

[3] C. Delande, M. Meynadier, and M. Voos, Phys. Rev. B **31**, 2497 (1985).

[4] J. Feldmann, G. Peter, E. Göbel, P. Dawson, K. Moore, C. Foxon, and R. Elliott, Phys. Rev. Lett. **59**, 2337 (1987).

[5] J. Kusano, Y. Segawa, Y. Aoyagi, S. Namba, and H. Okamoto, Phys. Rev. B **40**, 1685 (1989).

[6] P. Zhou, H. Jiang, R. Bannwart, S. Solin, and G. Bai, Phys. Rev. B **40**, 11 862 (1989).

[7] H. Jiang, E. Ping, P. Zhou, and J. Lin, Phys. Rev. B **41**, 12 949 (1989).

[8] M. Zachau, J. Kash, and W. Masselink, Phys. Rev. B **44**, 8403 (1991).

[9] B. Deveaud, F. Clerot, N. Roy, K. Satzke, B. Sermage, and D. Katzer, Phys. Rev. Lett. **67**, 2355 (1991).

[10] D. Oberhauser, K. Pantke, J. Hvam, G. Weismann, and C. Klingshirn, Phys. Rev. B **47**, 6828 (1993).

[11] J. Martinez-Pastor, A. Vinattieri, L. Carraresi, M. Colocci, P. Roussignol, and G. Weimann, Phys. Rev. B **47**, 10 456 (1993).

[12] Y. Takahashi, S. Kano, K. Muraki, S. Fukatsu, Y. Shiraki, and R. Ito, Appl. Phys. Lett. **64**, 1845 (1994).

[13] H. F. Hess, E. Betzig, T. D. Harris, L. N. Pfeiffer, and K. W. West, Science **264**, 1740 (1994).

[14] K. Fujiwara, H. Katahama, K. Kanamoto, R. Cingolani, and K. Ploog, Phys. Rev. B **43**, 13 978 (1991).

[15] K. Fujiwara, K. Kanamoto, N. Tsukada, H. Miyatake, and H. Koyama, J. Appl. Phys. **66**, 1488 (1989).

[16] K. Fujiwara, K. Kanamoto, and N. Tsukada, Phys. Rev. B **40**, 9698 (1989).

[17] U. Jahn, K. Fujiwara, J. Menniger, and H. T. Grahn, J. Appl. Phys. **77**, 396 (1995).

[18] R. Eccleston, R. Strobel, W. Rühle, J. Kuhl, B. Feuerbacher, and K. Ploog, Phys. Rev. B **44**, 1395 (1991).

[19] P. Roussignol, C. Delande, A. Vinettieri, L. Carraresi, and M. Colocci, Phys. Rev. B **45**, 6965 (1992).

[20] In Fig. 2 the dynamics is shown for three orders of magnitude, in contrast to the linear scale in Fig. 4. For the spectral evolution the dynamic range is limited by the spectral width (2 meV) of the free- and bound-exciton emission line compared to the peak separation of 3 meV to one order of magnitude.